# Effect of Plant Aggregates on Mechanical Properties of Earth Bricks

Aurélie Laborel-Préneron, Jean-Emmanuel Aubert, Camille Magniont, Pascal Maillard, C. Poirier

# Effect of plant aggregates on mechanical properties of earth bricks

A. Laborel-Préneron[1*], J-E. Aubert[2], C. Magniont[3], P. Maillard[4], C. Poirier[5]

[1] *LMDC, INSA/UPS Génie Civil, 135 Avenue de Rangueil, 31077 Toulouse cedex 04 France.*

[2] *LMDC, INSA/UPS Génie Civil, 135 Avenue de Rangueil, 31077 Toulouse cedex 04 France.*

[3] *LMDC, INSA/UPS Génie Civil, 135 Avenue de Rangueil, 31077 Toulouse cedex 04 France.*

[4] *Centre Technique de Matériaux Naturels de Construction (CTMNC), Service Céramique R&D, Ester Technopole, 87069 Limoges Cedex, France*

[5] *Centre Technique de Matériaux Naturels de Construction (CTMNC), Service Céramique R&D, Ester Technopole, 87069 Limoges Cedex, France*

alaborel@insa-toulouse.fr

aubert@insa-toulouse.fr

c_magnio@insa-toulouse.fr

p.maillard@ctmnc.fr

c.poirier@ctmnc.fr

*Corresponding author: Aurélie Laborel-Préneron

Tel. +33 (0)5 61 55 99 26 Fax: 0033 (0)5 61 55 99 49;

e-mail: alaborel@insa-toulouse.fr

# Effect of plant aggregates on the mechanical properties of earth bricks


## ABSTRACT

A building material is mainly characterized by its mechanical performance, which provides proof of its quality. However, the measurement of the compressive or flexural strength of an earth-based material with plant aggregates, which is very ductile, is not fully standardised. The objective of this study is to determine the compressive and flexural strengths of a composite made of earth and 0%, 3% or 6% of barley straw, hemp shiv or corn cob. Given the manufacturing processes available, cylindrical compressed specimens were studied in compression whereas extruded specimens were studied in flexion. Two protocols were tested for compressive strength measurements: one with direct contact between the specimen and the press, and the other with reduced friction. The test with reduced friction engendered a huge decrease of the stress and a slight decrease of the strain. For both compressive and flexural strengths, the specimens made of earth alone were the most resistant, followed by composites containing straw. The influence of two different treatments applied to the straw is also discussed.



Keywords: mechanical properties, earth blocks, straw, hemp shiv, corn cob, extrusion


## INTRODUCTION

The building sector is currently innovating in order to use more environmentally friendly materials and to ensure the comfort of users. To this end, it is developing new ecological materials (such as lightweight concrete (Chabannes et al., 2014; Magniont, 2010), or concrete using wastes (Palankar et al., 2015)) but it is also

looking into older, traditional ways, focusing on materials such as earth, stone or wood.

Nowadays, around 30% of the world's population still lives in earth shelters, especially in developing countries (Minke, 2006). Earth is a local resource that is available in abundance and presents many other advantages. This material has low environmental impact because of its recyclability, the little energy needed for the transformation process, the minimal transport required and its energy efficiency. Moreover, it is able to regulate indoor moisture and to improve the comfort of the building’s users (Islam and Iwashita, 2006; Minke, 2006).

However, earth material presents some weaknesses, such as low mechanical strength, brittleness, hygroscopic shrinkage and limited durability with respect to water (Aymerich et al., 2012; Islam and Iwashita, 2006). In order to reduce these drawbacks, some authors have studied the effect of adding stabilizers such as hydraulic binders and artificial or natural fibres or aggregates (Danso et al., 2015a; Laborel-Préneron et al., 2016). The enhancement of soil blocks by stabilizers was reviewed by Danso et al. (Danso et al., 2015a), especially concerning mechanical and water absorption properties. The interest of adding plant aggregates was also highlighted by Laborel-Préneron et al. (Laborel-Préneron et al., 2016). Based on empirical knowledge, the use of natural fibres and excrement has always helped to improve the properties of earth for building (Chazelles et al., 2011; Millogo et al., 2016). Such additions are now being increasingly studied within an earth matrix because of their apparently huge potential to improve thermal insulation (Bal et al., 2013) and ductility (Mostafa and Uddin, 2015) among other properties.

The present paper deals only with the mechanical properties of earth blocks containing plant aggregates. These properties are indeed essential if the material under study is to be used for construction purposes. They will determine whether

it can be used in a load bearing structure or not. However, the mechanical requirements vary from one standard to another, as do the testing procedures, which makes the characterization of this kind of material difficult. In the literature, many studies focus on the influence of plant fibres or aggregates on compressive strength. Twenty-three references investigating compressive strength on this kind of materials are cited in (Laborel-Préneron et al., 2016). Several studies have observed an increase of compressive strength with increasing proportions of plant aggregates such as tea residue (Demir, 2006), sawdust, tobacco residue or grass (Demir, 2008) or cassava peel (Villamizar et al., 2012). However, others have found a decrease in strength: Algin et al. showed a 71% compressive strength decrease with the addition of 7% of cotton waste (Algin and Turgut, 2008), and a decrease was also observed with straw (Mohamed, 2013) or coconut fibres (Khedari et al., 2005). In some cases, the effect of fibre length was studied. According to Millogo et al. (Millogo et al., 2014, 2015), the compressive strength of the earth composite increased by as much as 16% with the addition of short Hibiscus Cannabinus fibres (3 cm) but decreased with long ones (6 cm), except for a content of 0.4%. An influence of the aspect ratio was also observed by Danso et al. (Danso et al., 2015b) for coconut, bagasse and oil palm fibre, but with an increase of compressive strength as the length of the added fibres increased. None of these studies on earth material with plant aggregates deal with the influence of the testing protocol. However, Morel et al. (Morel et al., 2007) reviewed the various existing protocols for compressive strength testing of blocks of earth alone. Aubert et al. (Aubert et al., 2013, 2015) have discussed the testing of extruded earth blocks, considering the influence of: aspect ratio, confinement (capping with Teflon or not), anisotropy and the mortar joint between two half blocks, on the compressive strength measurement.

104 Several references focus on the flexural strength of these materials. An increase
105 in flexural strength is observed in most of the studies with an addition of plant
106 aggregates, e.g. Bouhicha et al. (Bouhicha et al., 2005) with barley straw or
107 Aymerich et al. (Aymerich et al., 2012) with wool fibres, but others have observed
108 a decrease, e.g. Villamizar et al. with cassava peels (Villamizar et al., 2012). In all
109 cases, ductility is greatly improved, as the fibre bridging of microcracks prevents
110 them from expanding (Galán-Marín et al., 2010; Mattone, 2005; Mostafa and
111 Uddin, 2015; Segetin et al., 2007).
112 A few, relatively recent, works have investigated the energy absorbed and the
113 mode of failure (Aymerich et al., 2016; Islam and Iwashita, 2006; Lenci et al.,
114 2012; Martins et al., 2014). In flexion, failure usually occurs by fibre gradually
115 slipping from the matrix, leading to both pull out and breaking of the fibres
116 (Mostafa and Uddin, 2015). Some authors have treated the fibres in an attempt to
117 improve the adhesion between the fibre and the matrix and thus enhance the
118 flexural or tensile strength. Some encouraging results have been obtained,
119 notably with acetylation, depending on the temperature of the chemical reaction
120 (Hill et al., 1998), or alkaline treatments on sisal fibres (Alvarez and Vázquez,
121 2006) or banana fibres (Mostafa and Uddin, 2015). However, a linseed oil
122 treatment used by Ledhem et al. on wood shavings gave less promising results,
123 with a decrease in strength, especially in traction.
124 The material studied in this paper is a bio-composite composed of earth and
125 three different plant aggregates: barley straw, hemp shiv and corn cob.
126 Composite specimens were manufactured according two processes:
127 compression or extrusion. After characterization of the earth used, the influence
128 of plant aggregate content on compressive strength and flexural strength was
129 analysed. Compressed specimens were tested in compression following two
130 protocols, one with friction and the other using a system to reduce friction. The

extruded specimens were tested in flexion. The effects of various treatments on barley straw and the effect of its aspect ratio were investigated with this test. The fracture energy developed during the test was also calculated.

## MATERIALS AND METHODS

### Raw materials

*Earth*

Earth used in this study was composed of quarry fines from aggregate washing processes (FWAS). These fines, smaller than 0.1 mm, were generated by the washing of limestone aggregates produced for the chemical or concrete industry. The sludge created was left to dry in sedimentation basins and was then reduced to powder to be used in different applications.

*Plant aggregates*

Three types of plant aggregates were used in this study: barley straw (two different lengths), hemp shiv and corn cob. Barley Straw (S) is the part of cereal's stem rejected during the harvest. Hemp shiv (H) is the by-product of the hemp defibration process and corresponds to the lignin-rich part of the stem. Corn Cob (CC) is the central part of the ear of corn cleared of grain and crushed. The hardest part was studied here. The physical and chemical characteristics of these plant aggregates were determined in (Laborel-Préneron et al., 2017) and are recapitulated in Table 1. However, the previous characterization was done only for the shortest straw ($S_{short}$), of average length 8 mm. In the present study, the longest straw ($S_{long}$), of average length 15 mm, was used only for the flexural strength test.

***Insert Table 1 here***

*Surfactant additives*

158 In agriculture, the efficiency of crop protection products can be improved by the
159 addition of surfactants that increase the absorption of the product on the plants.
160 These additives can optimize spreading and reduce negative effects such as drift
161 and run off. In this study, the objective of using these surfactants was to increase
162 the adhesion between the plant aggregates and the earth matrix by reducing the
163 surface tension of the mixing water. Two types of surfactant additives were
164 tested: A1, which was soya lecithin based, and A2, which was latex based. They
165 were both applied to the long straw only.
166 To apply the surfactants to the straw, the particles were immersed for 1 hour in
167 the additive, diluted at the rate recommended by the supplier: 0.5% of the water
168 volume for A1 and 0.1% for A2. The straw was then sieved to remove extra water
169 before being dried at 30°C in an oven.
170
171 **Physical, chemical and mineralogical characterization of FWAS**
172 *Particle size distribution and Atterberg limits*
173 The size distribution was determined by sedimentation after wet sieving at 80 µm,
174 according to standard NF P94-057 (AFNOR, 1992). The geotechnical
175 characteristics were evaluated using the Atterberg limits, according to standard
176 NF P 94-051 (AFNOR, 1993).
177
178 *Chemical and mineralogical composition*
179 X-ray diffraction on a sample crushed to a size of less than 80 µm was carried
180 out with a Siemens D5000 powder X-ray diffractometer equipped with a
181 monochromator having a Ka (λ=1.789Å) cobalt anticathode. Thermal
182 mineralogical characterization was also performed by thermal gravimetric
183 analysis (TGA) of a crushed sample (< 80 µm) heated to 1050°C at a constant
184 rate of 10°C.min$^{-1}$. Major oxide composition was evaluated on the basis of

185 macroelemental analysis performed by Inductively Coupled Plasma-Atomic
186 Emission Spectrometry (ICP-AES) on crushed samples smaller than 80 µm. The
187 mineral composition was determined from X-ray diffraction results and the
188 chemical composition.
189
190 **Manufacturing process**
191 Specimens for the different tests were prepared by two manufacturing processes:
192 one using static compression and the other using extrusion. The proportion of
193 plant aggregates was expressed by dry weight content, according to formula (1):

$$Ag.content = \frac{m_{Ag}}{m_{Ag} + m_{FWAS}} \times 100 \quad (1)$$

194 where Ag. content is the plant aggregate content in %, $m_{Ag}$ is the dry mass of
195 plant aggregates and $m_{FWAS}$ is the dry mass of earth.
196
197 *Compressed specimens*
198 Various mixtures were prepared to make the specimens: FWAS only and
199 mixtures containing one of the plant aggregates in a proportion of 3% or 6%. The
200 water contents of the mixtures were determined by the Proctor test, and then
201 rounded up because, according to Minke (Minke, 2006), this is a minimum value
202 for manufacturing compressed earth bricks.

Table **2** recapitulates the different mixture proportions and the dry densities of the specimens obtained (average of six specimens). As expected, the water content of the dry mass needed to make the mixtures increased when the plant aggregate content increased. It was higher for straw than for hemp and corn cob because straw particles have a higher water absorption coefficient than the other two aggregates (414% vs. 380% for hemp and 123% for corn cob) (Laborel-Préneron et al., 2017).

***Insert table 2 here***

To manufacture the specimens, the earth and plant aggregate fractions were poured into a blender and mixed by hand. Then, water was added and the materials were mixed mechanically until a homogeneous mix was obtained. The raw materials were mixed the day before moulding.

Cylindrical specimens 5 cm in diameter and 5 cm high (Φ5H5), intended for compressive strength tests, were manufactured by double static compression at the Proctor density. After demoulding, the height of the specimens containing barley straw and hemp shiv increased significantly due to the high compressibility of the plant aggregates. This increase reached 10% of the height for an addition of 6% of hemp shiv, for example. This expansion led to the formation of distributed cracks, specifically in the case of an addition of 6% of straw (Figure 1). The specimens were first dried at 40°C for 24 hours, then the temperature was increased by 0.1°C/min to 100°C and kept at 100°C until the weight became constant (weight variation less than 0.1% between two weighings 24 hours apart). This rise in temperature was carried out slowly to keep shrinking homogeneous and to avoid mechanical stresses. The specimens were then stored in a room regulated at 20°C and 50% relative humidity (RH) and were

tested when they were in equilibrium with the environment (about one week later).

***Figure 1. Compressed specimens of FWAS (a) and S6 (b)***

*Extruded specimens*

Six types of specimens were prepared: specimens made with FWAS only (i), and specimens made with 3% of short straw (ii), long straw (iii), hemp shiv (iv), long straw treated with the A1 surfactant (v), or long straw treated with the A2 surfactant (vi). Corn cob was not tested in extrusion because of the poor distribution of the particles observed in a preliminary trial and its low strength in compression. To manufacture these specimens, earth and plant aggregate fractions were poured into a blender and were mixed by hand. Then, the materials were mixed mechanically in the blender and water was added progressively until the consistency of the mixture was sufficiently homogeneous and plastic to be extruded. The details of the mixes are recapitulated in

**Table 3**.

***Insert table 3 here***

The specimens were manufactured with a medium sized laboratory extruder. The mixture was extruded under vacuum through a 7 cm x 3.5 cm die (Figure 2). The specimens were difficult to cut in the fresh state because of the presence of plant particles. They were therefore air-dried until the weight become constant (weight variation of less than 0.1% between two weighings 24 hours apart) and then cut to a length of 18 cm with a circular saw. Treatment of the straw did not modify the dry density of the composites. However, when the two manufacturing processes were compared (

255 Table **2** and

256

**Table 3**), an increase of density was observed for the extruded specimens containing plant aggregates. It was due to the extrusion of the material under vacuum, which reduced porosity, and to the extrusion pressure due to the worm screw.

***Figure 2. Vacuum extruder***

**Compressive strength test**

The compressive strength tests on the Φ5H5 specimens were performed using a 100 kN capacity hydraulic press. The load was applied at a constant deflection rate of 3 $mm.min^{-1}$. This speed was chosen as an intermediate value between the 1.2 $mm.min^{-1}$ specified in the French standard XP P 13-901 (AFNOR, 2001) (intended for compressed earth blocks) and the 5 $mm.min^{-1}$ used by Cerezo (Cerezo, 2005) (intended for hemp concrete). Three specimens of each mixture were tested in two different tests: one test with the specimen in direct contact with the steel plates (generating friction) and the other including a system avoiding friction (Figure 3) as described by Olivier et al. (Olivier et al., 1997). In the latter case, a 2-mm-thick piece of Teflon and a thin neoprene sheet - with a drop of oil between the layers - were placed between the earth specimen and the steel (neoprene in contact with the specimen, and Teflon in contact with the steel). Teflon was used because of its low friction coefficient and neoprene because of its high mechanical resistance. Displacements and loads were measured in each case. The Young's modulus of each specimen was then calculated from the linear part of the stress-strain curve.

***Figure 3. Compressive test method: (a) with friction and (b) with reduced friction***

**Flexural strength test**

The flexural strength tests on the extruded specimens were performed using a 100 kN capacity hydraulic press with a 10 kN sensor. The load was applied at a

constant deflection rate of 1 mm.min$^{-1}$ as was done by Aymerich et al. (Aymerich et al., 2012). The samples were loaded under three point loading conditions with the lower supports placed 10 cm apart, corresponding to the value given in the French standard NF EN 196-1 intended for cements (AFNOR, 2006). Measurements were made in triplicate.

This test was carried out in order to study the effect of the plant aggregate addition on ductility. According to the literature, this kind of addition has a marked effect on ductility (Aymerich et al., 2012; Bouhicha et al., 2005; Galán-Marín et al., 2010; Ghavami et al., 1999). Deflection was measured from bottom to top on an aluminium platelet glued in the middle of the sample, as can be seen on Figure 4. The test was stopped for a deflection close to 3 mm, the limit of the sensor stroke.

***Figure 4. Flexural test set up***

In order to compare the flexural strength with values reported in the literature or values from standards, the bending stress was calculated only at failure with the beam theory. Considering that classical hypotheses of solid mechanics applied and that the section was not cracked until peak load (elastic part of the curve) (Lenci et al., 2012; Mostafa and Uddin, 2015), the stress $\sigma$ (MPa) was calculated from the following expression (2):

$$\sigma = \frac{3FL}{2bh^2} \quad (2)$$

with F the maximum load at failure (N), L the distance between the supports (mm), b the width (mm) and h the height (mm) of the sample.

To determine the effect of the plant aggregate on the behaviour at failure and post-peak, the fracture energy ($G_f$) was calculated. It provided information about

the amount of energy absorbed when the specimen was broken into two parts. It was represented by the area under the load-displacement curve divided by the projected fracture area (Guinea et al., 1992). Usually, it is measured on notched samples (Aymerich et al., 2012, 2016; Guinea et al., 1992), so the whole load-displacement curve is considered. However, as the samples did not have a notch, the area was taken into account from the failure point and to a deflection of 3 mm. The fracture energy was calculated from the expression (3):

$$G_f = \frac{\int_{\delta_f}^{\delta_{3mm}} F(\delta)}{S} \quad (3)$$

where $\delta_f$ is the deflection at failure (m), F is the load (N) and S is the initial section ($m^2$).

The Young's modulus of each specimen was then calculated from the linear part of the stress-strain curve.

## RESULTS AND DISCUSSION

### Characterization of earth

*Particle size distribution and Atterberg limits*

The particle size distribution is presented in Figure 5 and compared with the size distribution recommended for compressed earth blocks (CEB) in the XP 13-901 standard (AFNOR, 2001).

***Figure 5. Comparative grain size distribution curve for earth: FWAS and standard***

The earth was extremely fine: 99% of the particles were smaller than 80 µm and the average particle size (D50) determined using the pipette analysis was 6.5 µm. The curve did not fit the limits recommended by the standard, the passing mass being higher for each grain size. Atterberg limits were equal to 30% for the liquid limit, 21% for the plastic limit and 9% for the plasticity index. The plasticity

of this material was not located in the spindle of the diagram recommended by the XP 13-901 standard (AFNOR, 2001). However, even though the size distribution and Atterberg limits did not meet the recommended criteria, it was already shown that it was possible to manufacture CEBs with a huge variety of earths (Aubert et al., 2014; Laborel-Préneron et al., 2016).

*Chemical and mineralogical composition*

The X-ray diffractogram is presented on Figure 6. This diagram reveals the large presence of calcite ($CaCO_3$) and shows the presence of other minerals in smaller quantities: kaolinite ($Al_2Si_2O_5(OH)_4$), quartz ($SiO_2$), illite ($KAl_2(AlSi_3)O_{10}(OH)_2$), goethite (FeO(OH)) and dolomite ($CaMg(CO_3)_2$).

***Figure 6. X-ray diffraction pattern of the earth. (c) calcite, (d) dolomite, (g) goethite, (i) illite, (k) kaolinite, (q) quartz***

To complete its mineralogical characterization, the earth was subjected to thermal gravimetric analysis, the results of which are presented in Figure 7. The loss of mass around 105°C was due to the evaporation of water and that around 540°C indicated the removal of the constituting water, which led to the transformation of kaolinite into metakaolinite (Kornmann and Lafaurie, 2005). The greatest loss of weight, of about 25%, occurred around 910°C and was due to the decarbonation of calcite and dolomite.

***Figure 7. TG and DTG (Derivative Thermo-Gravimetric) curves of the earth***

The chemical composition of the earth is given in

Table **4**, where a large amount of calcium is noticeable. Using the chemical composition and the mineral characterization, it is possible to estimate the proportion of each mineral. The fines used were thus composed for 60% of calcite, 11% of kaolinite, 11% of illite, 10% of quartz, 6% of dolomite and 3% of goethite.

***Insert table 4 here***

**Compressive strength measured on compressed specimens**

The average over three specimens of dry density, maximum compressive strength and other mechanical properties of each mixture and for each testing protocol are reported in

Table 5. The compressive strength value required by the New-Zealand Earth Building standard NZS 4298 (NZS 4298) is 1.3 MPa. This value was reached for all the mixtures of this study, for both protocols, except for CC6 tested with reduced friction (0.9 MPa).

***Insert table 5 here***

*Influence of plant aggregate type and content on the bulk density*

A number of authors have shown that bulk density is influenced by the addition of plant aggregates (Algin and Turgut, 2008; Demir, 2008; Khedari et al., 2005). The bulk density of each mixture used here is plotted on Figure 8. As expected, bulk density decreased as the aggregate content increased for the three kinds of plant aggregates. However, some differences between the mixtures with straw or hemp and the mixture with corn cob can be noted. Bulk density was higher for the mixtures with corn cob than for those with straw or hemp. This difference may have been due to the huge variability of the particle bulk densities: 497 $kg.m^{-3}$ for corn cob against 57 $kg.m^{-3}$ and 153 $kg.m^{-3}$ for straw and hemp shiv, respectively (Laborel-Préneron et al., 2017).

***Figure 8. Bulk density as a function of the plant aggregate content***

*Influence of the testing protocol on compressive strength*

Usually, only the compressive test with friction is performed ((Galán-Marín et al., 2010; Mohamed, 2013; Villamizar et al., 2012)) and follows standards ASTM D2166 (ASTM D 2166, 2004), XP P 13-901 (AFNOR, 2001) or TS EN 772-1 (TS EN 772-1, 2002). However some authors have also measured the strength with lower friction (using a layer of sand and a transparent film on either side of the sample (Piattoni et al., 2011; Quagliarini and Lenci, 2010) or with Teflon (Aubert et al., 2015)) to obtain the "real" compressive strength. Both methods, with friction and with Teflon reducing friction, were carried out to see what difference was actually observed. The results are shown in Figure 9.

***Figure 9. Compressive strength of the mixtures according to the testing protocol***

For each composition, the compressive strength measured in the tests with friction was greater than that found in tests with reduced friction because of the confinement (transverse displacements not allowed at the ends of the specimens). In the case of earth alone (FWAS) and S6 specimens, the decrease in strength between the protocols was only about 3 to 5%, whereas it reached between 28% (C6) and 59% (CC3) for the other mixtures. In some cases (FWAS or CC6), standard deviation was quite high. In the case of CC6, for example, this large variability of the results was due to one specimen having significantly higher strength than the other two - probably because of the heterogeneity of the material (Aubert et al., 2015), with a poor distribution of the corn cob granules. The results of H3, H6, CC3 and CC6 measured with reduced friction are very close; it is thus difficult to establish the highest strength with this protocol.

Unlike Aubert et al.'s finding (Aubert et al., 2015) that the strength decreased by only 10% with the use of Teflon capping, the choice of the method was observed to significantly affect the strength value measured here. It is thus important to choose the most adequate method. In order to allow comparisons among samples, and with the literature, only the values obtained with friction were kept here. This protocol was also easier to set up and more similar to the behaviour of a brick within a wall, with friction between the bricks.

*Effect of the plant aggregates on compressive strength*

The compressive strengths of the specimens are summarized in Figure 10 for the different plant aggregate types and contents when the protocol with friction at the interface between the specimen and the press was employed.

420 The compressive strength of the specimen composed of earth alone is higher
421 than that of all the others, which is in accordance with the density values of the
422 various specimens. Its average strength of 4.0 MPa is higher than the typical
423 value for CEBs which is, according to Morel et al. (Morel et al., 2007), between 2
424 and 3 MPa. Furthermore, a decrease in compressive strength is noticeable when
425 hemp shiv and corn cob contents increase. The values are 2.4 and 1.8 MPa for
426 H3 and H6, and 3.2 and 1.8 MPa for CC3 and CC6 specimens. This reduction,
427 linked to the incorporation of particles with low compressive strength and
428 stiffness, can be correlated to the decrease in bulk density observed with the
429 addition of plant aggregate (Al Rim et al., 1999; Ghavami et al., 1999). In the
430 case of barley straw, the average strengths are 3.3 MPa and 3.8 MPa for S3 and
431 S6 respectively. The ultimate compressive strength of S6 specimens is thus
432 higher than that of S3 specimens. This can be explained by a consolidation
433 phenomenon due to the high compressibility of the straw that allows its porosity
434 to decrease as strain increases. This phenomenon is not observed for H6 or CC6
435 specimens because of the lower ductility of hemp and corn aggregates. This
436 difference could also be due to the different shapes of the particles, straw being
437 more elongated than hemp shiv (Laborel-Préneron et al., 2017). This kind of
438 result was also observed by Millogo et al. (Millogo et al., 2014) for the longest
439 fibres but for smaller quantities (less than 1%). This observation was explained
440 by the limitation of crack opening by the fibres.

441 ***Figure 10. Results for compressive strength test with friction***

442 *Effect of the plant aggregates on ductility*

443 Figure 11 shows the stress-strain curves of all the specimens. It can be noted
444 that FWAS specimens show brittle failure whereas the ultimate strain is high for
445 the specimens containing plant aggregates, especially those with 6%. Their peak
446 strain is, on average, 19.9, 10.7 and 2.5% for S6, H6 and CC6, respectively,

whereas it is only 1.3% for FWAS. Although these specimens are weaker than FWAS specimens, they are also more ductile, with a larger zone of plasticity. Ductility of the composite is thus increased by the addition of plant aggregates. However, in calculating building structures, such deformations of the material cannot be tolerated.

In order to make comparisons among the materials and to maintain a strain level compatible with the intended use, we chose to limit the strain to 1.5% and to keep the corresponding compressive strength value, as described by Cerezo (Cerezo, 2005) for hemp concrete. The maximum compressive strength was kept in cases when the failure occurred before 1.5% strain (which only concerned FWAS specimens).

These values are compared with the values at failure in Figure 12. For a given deformation, compressive strength is higher for FWAS specimens. The values are far below the maximum compressive strength and do not reach 1 MPa for the specimens with straw or hemp shiv whereas the compressive strength is above the limit of 1.3 MPa in the case of corn cob. In the cases where the materials do not have the strength required to be used as bearing structures, they can be used as infill material in a wood structure or as a partition wall, for instance.

***Figure 11. Strain-stress diagram for all the specimens***

***Figure 12. Maximum compressive strength ($\sigma_c$) and compressive strength at 1.5% strain ($\sigma_{c,1.5}$%)***

*Influence of the testing protocol on Young's modulus*

Young's moduli were obtained from compressive strength tests and are recapitulated in Figure 13, according to the testing protocol. Friction does not seem to have any great influence on the modulus, which is of the same order of magnitude for both situations (with quite large standard deviations). The most

striking result visible in the figure is that the Young's modulus of FWAS specimens is the highest (around 500 MPa).

***Figure 13. Young's moduli of the materials for both protocols***

*Effect of the plant aggregates on Young's modulus*

The Young's modulus obtained from the tests with friction is represented according to the plant aggregate content in Figure 14. The Young's moduli of the specimens containing 3% of barley straw, hemp shiv and corn cob are respectively 62, 75 and 217 MPa. For an addition of 6%, the moduli are 31, 26 and 102 MPa respectively for barley straw, hemp shiv and corn cob. Specimens made with straw and with hemp shiv showed very similar stiffness for a given content. With a modulus of 439 MPa, FWAS specimens had the highest stiffness. For an increase of each plant aggregate content, there was a decrease in the Young's modulus. This result can be explained by the high compressibility of the plant particles (Cerezo, 2005) and is in agreement with various references (Al Rim et al., 1999; Chee-Ming, 2011; Piattoni et al., 2011; Quagliarini and Lenci, 2010) stating that the straw addition controls the plastic behaviour of the specimen through a lower homogeneity of the mixture. This decrease of Young's modulus could be linked with the density of the specimens as shown in Figure 15. An empiric exponential correlation between Young's modulus and dry density is found: $E = 0.3184 \exp(0.0035\rho_{dry})$ with $\rho_{dry}$ in kg.m$^{-3}$. Such a relation has already been proposed by Al Rim et al. for earth specimens with wood aggregates (Al Rim et al., 1999), but it was $E = 1127d^{3.142}$ with d the density of the dry material relative to the density of water.

***Figure 14. Young's modulus from compressive test as a function of the plant aggregate content***

***Figure 15. Young's modulus as a function of the density***

**Flexural strength measured on extruded specimens**

The average of dry density, the maximum flexural strength and other mechanical parameters are reported in

503 Table 6. The minimum flexural tensile stress required by the Masonry Standards
504 Joint Committee (MSJC) (Masonry Standards Joint Committee (MSJC), 2008)
505 (quoted in (Villamizar et al., 2012)) for clay and concrete blocks is 0.21 MPa.
506 Another value, of 0.65 MPa, is required by the British Standard BS 6073 (BS
507 6073, 1981) (quoted in (Algin and Turgut, 2008)) for building materials to be used
508 in structural applications. All the flexural strengths of the specimens tested in this
509 study are above these two minimum requirements, the lowest strength being 1.34
510 MPa, found for H3 specimens.

511 ***Insert table 6 here***

512 *Effect of the plant aggregate type on the flexural strength*

513 The maximum flexural strengths of the different mixtures are represented in
514 Figure 16 (a). FWAS has the highest flexural strength, followed by $S3_{short}$, $S3_{long}$
515 and H3, with values of 2053, 1900, 1776 and 1453 N respectively. This result
516 could be correlated with the respective densities: the lower the density, the lower
517 the flexural strength.

518 It can be seen that the flexural strength is higher for the specimens with short
519 straw than for those with long straw. This result is contrary to the findings of some
520 other authors (Danso et al., 2015b; Mostafa and Uddin, 2015), who stated that an
521 increase of the fibre length increased the embedded length and thus the
522 adhesion area, leading to an improvement in flexural strength. This result could
523 be explained by the fact that, for the same straw content, there are more particles
524 in a mix with short straw than with long straw, engendering a better distribution of
525 the particles in the matrix. Another explanation could be the existence of a length
526 limit, depending on the specimen size, above which the difficulty of dispersion
527 offsets the positive effect of the reinforcement. Moreover, after being extruded
528 under vacuum, the specimens with short straw presented a better visual surface

quality than the specimens with long straw. This could lead to a better adhesion between the earth and the straw, explaining the higher resistance.

Although most cases in the literature show an increase in flexural strength with an addition of plant aggregate ((Al Rim et al., 1999; Aymerich et al., 2012; Bouhicha et al., 2005; Galán-Marín et al., 2010)), an adverse effect (decrease of flexural strength) was found by Villamizar et al. (Villamizar et al., 2012) with an addition of cassava peels and by Algin and Turgut (Algin and Turgut, 2008) with an addition of cotton wastes. This could be due to the heterogeneity of the material or the weakness of the adhesion between the particles and the matrix (Yetgin et al., 2008).

***Figure 16. Influence of the plant aggregate on flexural behaviour: (a) Flexural load-carrying capacity, (b) Peak strain ($\varepsilon_f$), (c) Average fracture energy ($G_f$) and (d) Young's modulus***

*Effect of the plant aggregate type on ductility and Young's modulus*

At the end of the tests, reinforced specimens were not totally split into two parts (Figure 4) and extra manual force was necessary to separate them, whereas FWAS specimens were divided into two parts. Figure 17 presents typical load-deflection curves obtained during the bending test for the different samples. These curves clearly show that the addition of plant aggregates increases the ductility, increasing the deflection at failure and giving some residual strength.

Peak strain is represented in Figure 16 (b). As mentioned above, the strain is increased with the addition of plant aggregates, especially for long particles. The strain was 0.44 and 0.55% respectively for short and long straw. The lower value in the case of hemp shiv (0.31%) could be attributed to a morphological effect: the particle is indeed less elongated and so does not have as much surface area in contact with the earth matrix as the straw particle.

555 Figure 16 (c) represents the average fracture energy for each composition. The
556 value is close to 0 $J.m^{-2}$ for the FWAS specimens whereas the fracture energy of
557 the other specimens is higher: 296, 484 and 157 $J.m^{-2}$ respectively for $S3_{short}$,
558 $S3_{long}$ and H3. The addition of plant aggregates allows a huge increase in fracture
559 energy. The energy absorbed increases when the length of the fibre increases; it
560 is 39% higher with long than short straw, meaning that its residual strength is
561 greater. This result shows that the fracture response of materials reinforced with
562 plant aggregates or fibres is governed by mechanisms of toughening such as
563 fibre bridging and fibre pull-out (Aymerich et al., 2016). These effects occur only
564 for sufficient crack opening.

565 ***Figure 17. Typical load-deflection curves***

566 The experimental values of Young's moduli are presented in Figure 16 (d). As for
567 the elastic moduli from the compressive test, they seem to decrease with the
568 addition of plant aggregates.

569 This result is partially correlated with the literature. Although the flexural Young's
570 modulus of an earth material with wood aggregates increased with between 10
571 and 20% of addition, it decreased above 20% (Al Rim et al., 1999).

572 *Effect of the surfactant on the flexural strength, post-peak behaviour and Young's*
573 *modulus*

574 The behaviour under flexion of the mixtures with untreated and treated long straw
575 is represented on Figure 18. The increase in flexural load capacity between $S_{A2}$
576 and $S3_{long}$ is only about 3% and the standard deviations are high. The surfactant
577 has no effect on the flexural strength.

578 Peak strain is represented in Figure 18 (b). The strain decreases with the addition
579 of a surfactant, especially the A2 additive. Strain is 0.55, 0.49 and 0.36% for
580 $S3_{long}$, $S_{A1}$ and $S_{A2}$ respectively.

Figure 18 (c) represents also the average fracture energy for the untreated and treated compositions. $S3_{long}$ and $S_{A1}$ present similar values, of 482 and 462 $J.m^{-2}$, respectively but a small increase of 10% can be noticed for $S_{A2}$, with a fracture energy of 538 $J.m^{-2}$.

Experimental values of Young's moduli are presented in the Figure 18 (d). The elastic modulus is higher for the treated specimens, with values of 442 and 508 MPa for $S_{A1}$ and $S_{A2}$, respectively, whereas it is only 385 MPa for $S3_{long}$. The A2 additive again seems to be the more efficient of the two surfactants tested here, giving an increase in stiffness of about 24%.

Even though the flexural strength is not increased by the straw treatment, the stiffness of the material seems to be increased and the adhesion between the straw and the matrix should also be improved. Surfactant A2 seems to have a greater effect than A1. However, this is a preliminary study, which needs to be pursued further, in particular to optimize various parameters such as the dilution ratio, application method and drying temperature.

***Figure 18. Influence of the surfactants on flexural behaviour: (a) Flexural load-carrying capacity, (b) Peak strain ($\varepsilon_f$), (c) Average fracture energy ($G_f$) and (d) Young's modulus***

## CONCLUSION

The mechanical properties of compressed and extruded earth-based specimens were tested. These two ways of manufacturing led to different densities for the same formulation. However, compressive and flexural measurements were independent. Several main conclusions can be drawn concerning the influence of the various parameters such as the plant aggregate type, the protocol of the test or possible treatment. Concerning the compressive tests, the measurement with reduced friction gave a lower compressive strength and peak strain. This method

gives a more "realistic" resistance, but is still little used in the literature. At rupture, strength was higher in the case of straw addition, followed by hemp shiv and corn cob additions. For both compressive and flexural tests, the addition of plant aggregates decreased the strength but improved the ductility of the material, decreasing the Young's modulus. Concerning flexural strength, a better resistance was observed for short than for long straw, but a higher strain was noted for the longest straw. Strain at peak was lower when the straw was treated with the A2 additive, but with the flexural strength was the same.

Various works have shown the diversity of mechanical tests existing for earth bricks and these should be harmonized by means of more investigation and standardization. However, the testing of bio-based earth materials should not be forgotten as their behaviour is much more ductile and cannot be tested in the same way. Although the treatment with surfactants did not improve the mechanical strength of the composites, it did cause a slight decrease in the strain at rupture. More investigation is thus required to optimize its effect on strength, in particular concerning the treatment process (the dilution rate and details of the straw treatment method). In this work, compressed specimens were used to study the influence of plant aggregates and surfactant additives during compression tests whereas extruded specimens were tested in flexion. However, in further work it would be interesting to determine whether or not the adhesion between earth and fibre differs according to the process used: compression or extrusion.

ACKNOWLEDGEMENTS

The authors wish to thank the French National Research Agency - France (ANR) for funding project BIOTERRA - ANR - 13 - VBDU - 0005 Villes et Bâtiments Durables.

635

636 REFERENCES

637 AFNOR (1992). NF P94-057 - Analyse granulométrique des sols - Méthode par
638 sédimentation.

639 AFNOR (1993). NF P94-051 - Détermination des limites d'Atterberg - Limite de
640 liquidité à la coupelle - Limite de plasticité au rouleau.

641 AFNOR (2001). Blocs de terre comprimée pour murs et cloisons : définitions -
642 spécifications - méthode d'essais - condition de réception.

643 AFNOR (2006). Méthode d'essais des ciments - Détermination des résistances
644 mécaniques.

645 Al Rim, K., Ledhem, A., Douzane, O., Dheilly, R.M., and Queneudec, M. (1999).
646 Influence of the proportion of wood on the thermal and mechanical performances
647 of clay-cement-wood composites. Cem. Concr. Compos. *21*, 269–276.

648 Algin, H.M., and Turgut, P. (2008). Cotton and limestone powder wastes as brick
649 material. Constr. Build. Mater. *22*, 1074–1080.

650 Alvarez, V.A., and Vázquez, A. (2006). Influence of fiber chemical modification
651 procedure on the mechanical properties and water absorption of MaterBi-Y/sisal
652 fiber composites. Compos. Part Appl. Sci. Manuf. *37*, 1672–1680.

653 ASTM D 2166 (2004). Standard test method for unconfined compressive strength
654 of cohesive soil.

655 Aubert, J.E., Fabbri, A., Morel, J.C., and Maillard, P. (2013). An earth block with a
656 compressive strength higher than 45 MPa! Constr. Build. Mater. *47*, 366–369.

657 Aubert, J.-E., Marcom, A., Oliva, P., and Segui, P. (2014). Chequered earth
658 construction in south-western France. J. Cult. Herit. *16*, 293–298.

659 Aubert, J.E., Maillard, P., Morel, J.C., and Al Rafii, M. (2015). Towards a simple
660 compressive strength test for earth bricks? Mater. Struct.

661 Aymerich, F., Fenu, L., and Meloni, P. (2012). Effect of reinforcing wool fibres on
662 fracture and energy absorption properties of an earthen material. Constr. Build.
663 Mater. *27*, 66–72.

664 Aymerich, F., Fenu, L., Francesconi, L., and Meloni, P. (2016). Fracture
665 behaviour of a fibre reinforced earthen material under static and impact flexural
666 loading. Constr. Build. Mater. *109*, 109–119.

667 Bal, H., Jannot, Y., Gaye, S., and Demeurie, F. (2013). Measurement and
668 modelisation of the thermal conductivity of a wet composite porous medium:
669 Laterite based bricks with millet waste additive. Constr. Build. Mater. *41*, 586–
670 593.

671 Bouhicha, M., Aouissi, F., and Kenai, S. (2005). Performance of composite soil
672 reinforced with barley straw. Cem. Concr. Compos. *27*, 617–621.

673 BS 6073 (1981). Part 1: precast concrete masonry units, Specification for precast
674 concrete masonry units.

675 Cerezo, V. (2005). Propriétés mécaniques, thermiques et acoustiques d'un
676 matériau à base de particules végétales: approche expérimentale et modélisation
677 théorique. Institut National des Sciences Appliquées.

678 Chabannes, M., Bénézet, J.-C., Clerc, L., and Garcia-Diaz, E. (2014). Use of raw
679 rice husk as natural aggregate in a lightweight insulating concrete: An innovative
680 application. Constr. Build. Mater. *70*, 428–438.

681 Chazelles, C-A de, Klein, A., and Pousthomis, N. (2011). Les cultures
682 constructives de la brique de terre crue - Echanges transdiciplinaires sur les
683 constructions en terre crue - 3 (Espérou).

684 Chee-Ming, C. (2011). Effect of natural fibres inclusion in clay bricks: Physico-
685 mechanical properties. Geotech. Geol. Eng. *73*, 1–8.

686 Danso, H., Martinson, B., Ali, M., and Mant, C. (2015a). Performance
687 characteristics of enhanced soil blocks: a quantitative review. Build. Res. Inf. *43*,
688 253–262.

689 Danso, H., Martinson, D.B., Ali, M., and Williams, J. (2015b). Effect of fibre
690 aspect ratio on mechanical properties of soil building blocks. Constr. Build. Mater.
691 *83*, 314–319.

692 Demir, I. (2006). An investigation on the production of construction brick with
693 processed waste tea. Build. Environ. *41*, 1274–1278.

694 Demir, I. (2008). Effect of organic residues addition on the technological
695 properties of clay bricks. Waste Manag. *28*, 622–627.

696 Galán-Marín, C., Rivera-Gómez, C., and Petric, J. (2010). Clay-based composite
697 stabilized with natural polymer and fibre. Constr. Build. Mater. *24*, 1462–1468.

698 Ghavami, K., Toledo Filho, R.D., and Barbosa, N.P. (1999). Behaviour of
699 composite soil reinforced with natural fibres. Cem. Concr. Compos. *21*, 39–48.

Guinea, G.V., Planas, J., and Elices, M. (1992). Measurement of the fracture energy using three-point bend tests: Part 1—Influence of experimental procedures. Mater. Struct. *25*, 212–218.

Hill, C.A.S., Khalil, H.P.S.A., and Hale, M.D. (1998). A study of the potential of acetylation to improve the properties of plant fibres. Ind. Crops Prod. *8*, 53–63.

Islam, M.., and Iwashita, K. (2006). Seismic response of fiber-reinforced and stabilized adobe structures. In Proceeding of the Getty seismic adobe project 2006 Colloquium, (Los Angeles, USA: Getty Conservation Institute).

Khedari, J., Watsanasathaporn, P., and Hirunlabh, J. (2005). Development of fibre-based soil–cement block with low thermal conductivity. Cem. Concr. Compos. *27*, 111–116.

Kornmann, M., and Lafaurie, P. (2005). Matériaux de construction en terre cuite Fabrication et propriétés (Paris: Ed. Septima).

Laborel-Préneron, A., Aubert, J.E., Magniont, C., Tribout, C., and Bertron, A. (2016). Plant aggregates and fibers in earth construction materials: A review. Constr. Build. Mater. *111*, 719–734.

Laborel-Préneron, A., Magniont, C., and Aubert, J.-E. (2017) Characterization of barley straw, hemp shiv and corn cob as resources for bioaggregate based building materials. Waste Biomass Valorization, doi10.1007/s12649-017-9895-z.

Lenci, S., Clementi, F., and Sadowski, T. (2012). Experimental determination of the fracture properties of unfired dry earth. Eng. Fract. Mech. *87*, 62–72.

721 Magniont, C. (2010). Contribution à la formulation et à la caractérisation d'un
722 écomatériau de construction à base d'agroressources. PhD thesis in Civil
723 Engineering. Université Toulouse III - Paul Sabatier.

724 Martins, A.P.S., Silva, F.A., and Toledo Filho, R.D. (2014). Mechanical behavior
725 of self-compacting soil-cement-sisal fiber composites. Key Eng. Mater. *634*, 421–
726 432.

727 Masonry Standards Joint Committee (MSJC) (2008). Building code requirements
728 and specification for masonry structures.

729 Mattone, R. (2005). Sisal fibre reinforced soil with cement or cactus pulp in
730 bahareque technique. Cem. Concr. Compos. *27*, 611–616.

731 Millogo, Y., Morel, J.-C., Aubert, J.-E., and Ghavami, K. (2014). Experimental
732 analysis of pressed adobe blocks reinforced with Hibiscus cannabinus fibers.
733 Constr. Build. Mater. *52*, 71–78.

734 Millogo, Y., Aubert, J.-E., Hamard, E., and Morel, J.-C. (2015). How properties of
735 kenaf fibers from Burkina Faso contribute to the reinforcement of earth blocks.
736 Materials *8*, 2332–2345.

737 Millogo, Y., Aubert, J.-E., Séré, A.D., Fabbri, A., and Morel, J.-C. (2016). Earth
738 blocks stabilized by cow-dung. Mater. Struct. *49*, 4583–4594.

739 Minke, G. (2006). Building with earth: design and technology of a sustainable
740 architecture (Basel, Switzerland).

741 Mohamed, A.E.M.K. (2013). Improvement of swelling clay properties using hay
742 fibers. Constr. Build. Mater. *38*, 242–247.

743 Morel, J.-C., Pkla, A., and Walker, P. (2007). Compressive strength testing of
744 compressed earth blocks. Constr. Build. Mater. *21*, 303–309.

745 Mostafa, M., and Uddin, N. (2015). Effect of banana fibers on the compressive
746 and flexural strength of compressed earth blocks. Buildings *5*, 282–296.

747 NZS 4298 Materials and workmanship for earth buildings.

748 Olivier, M., Mesbah, A., El Gharbi, Z., and Morel, J.C. (1997). Mode opératoire
749 pour la réalisation d'essais de résistance sur blocs de terre comprimée: Test
750 method for strength tests on blocks of compressed earth. Mater. Struct. *30*, 515–
751 517.

752 Palankar, N., Ravi Shankar, A.U., and Mithun, B.M. (2015). Studies on eco-
753 friendly concrete incorporating industrial waste as aggregates. Int. J. Sustain.
754 Built Environ. *4*, 378–390.

755 Piattoni, Q., Quagliarini, E., and Lenci, S. (2011). Experimental analysis and
756 modelling of the mechanical behaviour of earthen bricks. Constr. Build. Mater. *25*,
757 2067–2075.

758 Quagliarini, E., and Lenci, S. (2010). The influence of natural stabilizers and
759 natural fibres on the mechanical properties of ancient Roman adobe bricks. J.
760 Cult. Herit. *11*, 309–314.

761 Segetin, M., Jayaraman, K., and Xu, X. (2007). Harakeke reinforcement of soil–
762 cement building materials: Manufacturability and properties. Build. Environ. *42*,
763 3066–3079.

764 TS EN 772-1 (2002). Methods of test for mortar for masonry units - Part 1:
765 determination of compressive strength.

766 Villamizar, M.C.N., Araque, V.S., Reyes, C.A.R., and Silva, R.S. (2012). Effect of
767 the addition of coal-ash and cassava peels on the engineering properties of
768 compressed earth blocks. Constr. Build. Mater. *36*, 276–286.

769 Yetgin, Ş., Çavdar, Ö., and Çavdar, A. (2008). The effects of the fiber contents on
770 the mechanic properties of the adobes. Constr. Build. Mater. *22*, 222–227.

771 **Table 1.** Physicochemical properties of the plant aggregates

| Material | Barley straw | Hemp shiv | Corn cob |
|---|---|---|---|
| Designation | $S_{short}$ | H | CC |
| Bulk density ($kg.m^{-3}$) | 57.4 ± 1.2 | 153.0 ± 2.4 | 496.8 ± 14.0 |
| Water absorption (%) | 414 ± 4 | 380 ± 11 | 123 ± 2 |
| Diameter* (mm) | 2.33 ± 1.52 | 2.02 ± 1.23 | 2.63 ± 0.43 |
| Thermal conductivity ($W.m^{-1}.K^{-1}$) | 0.046 ± 0.001 | 0.053 ± 0.002 | 0.097 ± 0.001 |
| Chemical composition | | | |
| Lignin (%) | 5.5 | 17.2 | 6.6 |
| Cellulose (%) | 37.7 | 50.3 | 41.4 |
| Hemicellulose (%) | 26.7 | 17.9 | 40.7 |

772 * Corresponding to average minor axis by image analysis

773 **Table 2.** Mixture proportions and Proctor density of compressed specimens

| Reference | FWAS | S3 | S6 | H3 | H6 | CC3 | CC6 |
|---|---|---|---|---|---|---|---|
| Plant aggregate | - | Short straw | Short straw | Hemp | Hemp | Corn cob | Corn cob |
| Plant aggregate content (%) | 0 | 3 | 6 | 3 | 6 | 3 | 6 |
| Water content (%) | 14 | 19 | 21 | 17 | 20 | 16 | 16 |
| Dry density (kg.m$^{-3}$) | 1988±9 | 1520±1 | 1195±169 | 1553±69 | 1190±44 | 1877±2 | 1704±71 |

774

775

776 **Table 3.** Mixture proportions of extruded specimens

| Reference | FWAS | $S3_{short}$ | $S3_{long}$ | H3 | $S_{A1}$ | $S_{A2}$ |
|---|---|---|---|---|---|---|
| Plant aggregate | - | Short straw | Long straw | Hemp | Long straw | Long straw |
| Plant aggregate content (%) | 0 | 3 | 3 | 3 | 3 | 3 |
| Water content (%) | 20 | 24 | 26 | 25 | 24 | 25 |
| Surfactant | - | - | - | - | A1 | A2 |
| Dry density ($kg.m^{-3}$) | 1982±8 | 1781±10 | 1734±20 | 1712±11 | 1784±10 | 1782±12 |

777

778 **Table 4.** Chemical composition of the earth (LOI: Loss on Ignition)

| Oxides | $SiO_2$ | $Al_2O_3$ | $Fe_2O_3$ | MnO | MgO | CaO | $Na_2O$ | $K_2O$ | $TiO_2$ | $P_2O_5$ | LOI |
|---|---|---|---|---|---|---|---|---|---|---|---|
| % | 18.73 | 7.47 | 2.39 | 0.03 | 1.27 | 35.27 | 0.09 | 0.90 | 0.39 | 0.09 | 31.92 |

779

780 **Table 5.** Measured mechanical properties of the materials: dry density ($\rho_{dry}$) average compressive
781 strength ($\sigma_c$), average ultimate strain ($\varepsilon_c$), average compressive strength at 1.5% strain ($\sigma_{c,1.5\%}$) and
782 average experimental Young's modulus ($E_c$)

| Testing protocol | Reference | $\rho_{dry}$ (kg/m$^3$) | $\sigma_c$ (MPa) | $\varepsilon_c$ (%) | $\sigma_{c,1.5\%}$ (MPa) | $E_c$ (MPa) |
|---|---|---|---|---|---|---|
| With friction | FWAS | 1995 ± 0 | 4.0 ± 0.4 | 1.3 ± 0.1 | 4.0 ± 0.4 | 439 ± 54 |
| | S3 | 1519 ± 1 | 3.3 ± 0.2 | 7.8 ± 0.6 | 0.7 ± 0.1 | 62 ± 3 |
| | S6 | 1315 ± 27 | 3.8 ± 0.3 | 19.9 ± 1.1 | 0.4 ± 0.0 | 31 ± 1 |
| | H3 | 1603 ± 57 | 2.4 ± 0.2 | 4.8 ± 0.3 | 0.7 ± 0.1 | 75 ± 8 |
| | H6 | 1221 ± 70 | 1.8 ± 0.2 | 10.7 ± 3.1 | 0.4 ± 0.1 | 26 ± 3 |
| | CC3 | 1878 ± 1 | 3.2 ± 0.2 | 2.4 ± 0.2 | 2.1 ± 0.3 | 217 ± 45 |
| | CC6 | 1754 ± 13 | 1.8 ± 0.6 | 2.5 ± 0.5 | 1.3 ± 0.6 | 102 ± 69 |
| Reduced friction (RF) | FWAS | 1982 ± 10 | 3.9 ± 0.9 | 1.0 ± 0.1 | 3.9 ± 0.9 | 564 ± 161 |
| | S3 | 1520 ± 1 | 2.1 ± 0.2 | 5.6 ± 0.5 | 0.6 ± 0.0 | 43 ± 5 |
| | S6 | 1075 ± 30 | 3.6 ± 0.2 | 17.2 ± 1.5 | 0.3 ± 0.0 | 25 ± 0 |
| | H3 | 1504 ± 54 | 1.6 ± 0.1 | 3.6 ± 0.3 | 0.7 ± 0.1 | 51 ± 5 |
| | H6 | 1159 ± 41 | 1.5 ± 0.1 | 7.5 ± 1.1 | 0.4 ± 0.0 | 22 ± 1 |
| | CC3 | 1876 ± 1 | 1.3 ± 0.1 | 1.2 ± 0.1 | 1.3 ± 0.1 | 136 ± 40 |
| | CC6 | 1654 ± 53 | 1.0 ± 0.1 | 1.8 ± 0.2 | 0.9 ± 0.0 | 69 ± 9 |

783

784

785 **Table 6.** Average experimental mechanical properties: dry density ($\rho_{dry}$), flexural strength ($\sigma_f$),

786 ultimate strain ($\varepsilon_f$), experimental Young's modulus ($E_f$) and fracture energy ($G_f$)

| Type | $\rho_{dry}$ (kg.m$^{-3}$) | F (N) | $\sigma_f$ (MPa) | $\varepsilon_f$ (%) | $E_f$ (MPa) | $G_f$ (J.m$^{-2}$) |
|---|---|---|---|---|---|---|
| FWAS | 1982 ± 8 | 2053 ± 120 | 1.88 ± 0.10 | 0.22 ± 0.02 | 856 ± 57 | 7 ± 0 |
| $S3_{short}$ | 1781 ± 10 | 1900 ± 123 | 1.80 ± 0.13 | 0.44 ± 0.11 | 475 ± 49 | 296 ± 50 |
| $S3_{long}$ | 1734 ± 20 | 1776 ± 135 | 1.69 ± 0.14 | 0.55 ± 0.14 | 385 ± 29 | 484 ± 41 |
| H3 | 1712 ± 11 | 1453 ± 86 | 1.34 ± 0.08 | 0.31 ± 0.04 | 577 ± 72 | 157 ± 9 |
| $S_{A1}$ | 1784 ± 10 | 1798 ± 163 | 1.69 ± 0.16 | 0.49 ± 0.03 | 442 ± 72 | 462 ± 11 |
| $S_{A2}$ | 1782 ± 12 | 1824 ± 183 | 1.73 ± 0.10 | 0.36 ± 0.08 | 508 ± 67 | 538 ± 81 |

787

788

789 Figure 1. Compressed specimens of FWAS (a) and S6 (b)

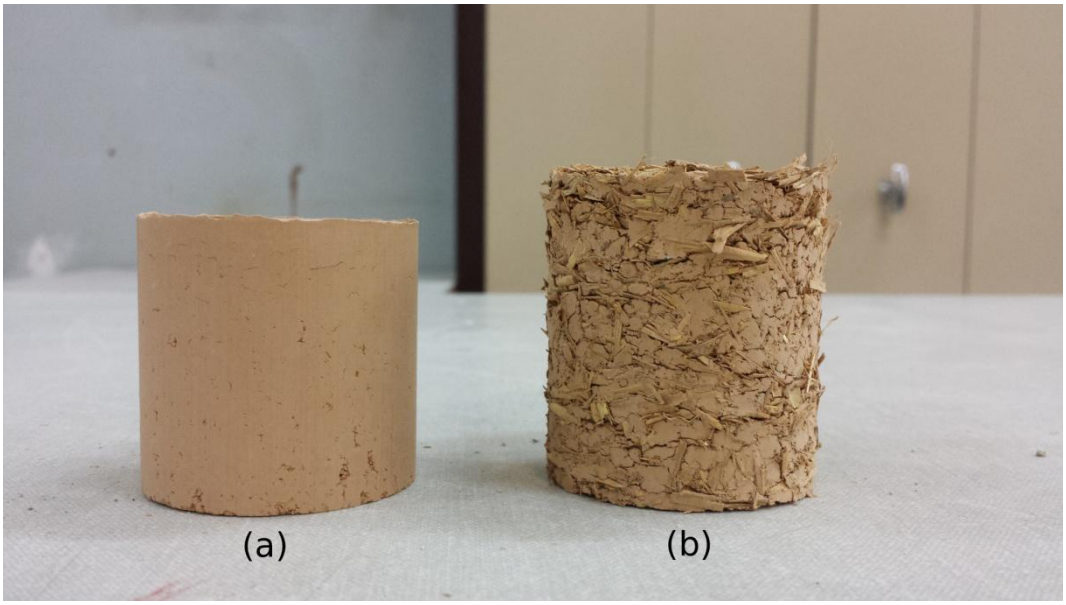


790
791

Figure 2. Vacuum extruder

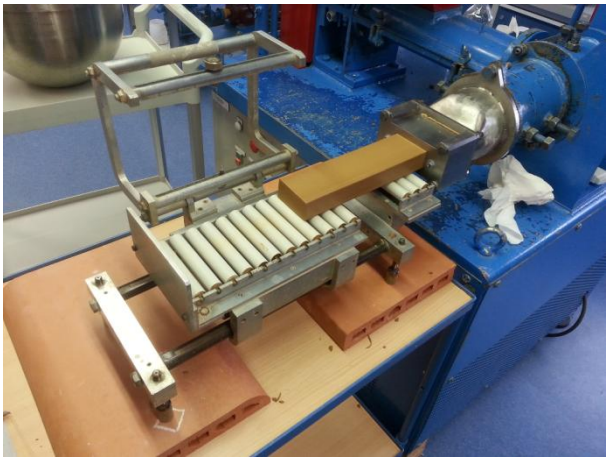

794 Figure 3. Compressive test method: (a) with friction and (b) with reduced friction

795 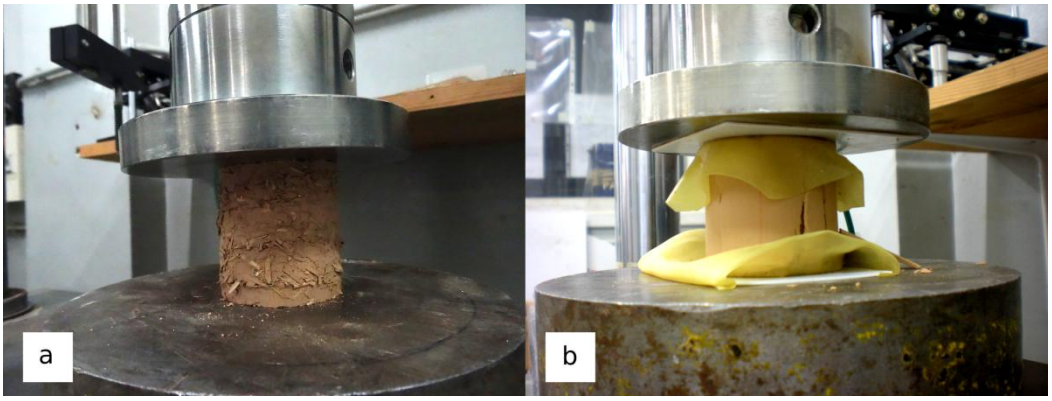

796 Figure 4. Flexural test set up

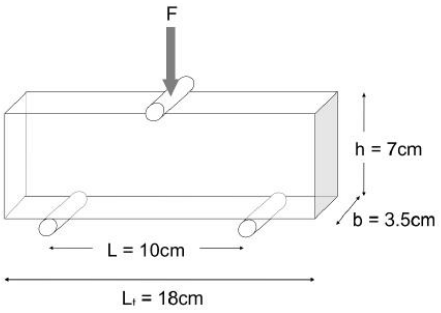


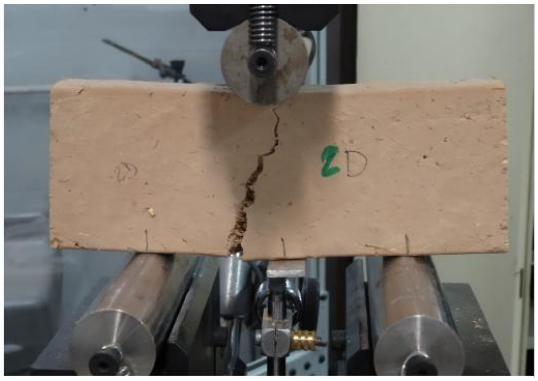

797
798

799 Figure 5. Comparative grain size distribution curve for earth: FWAS and standard

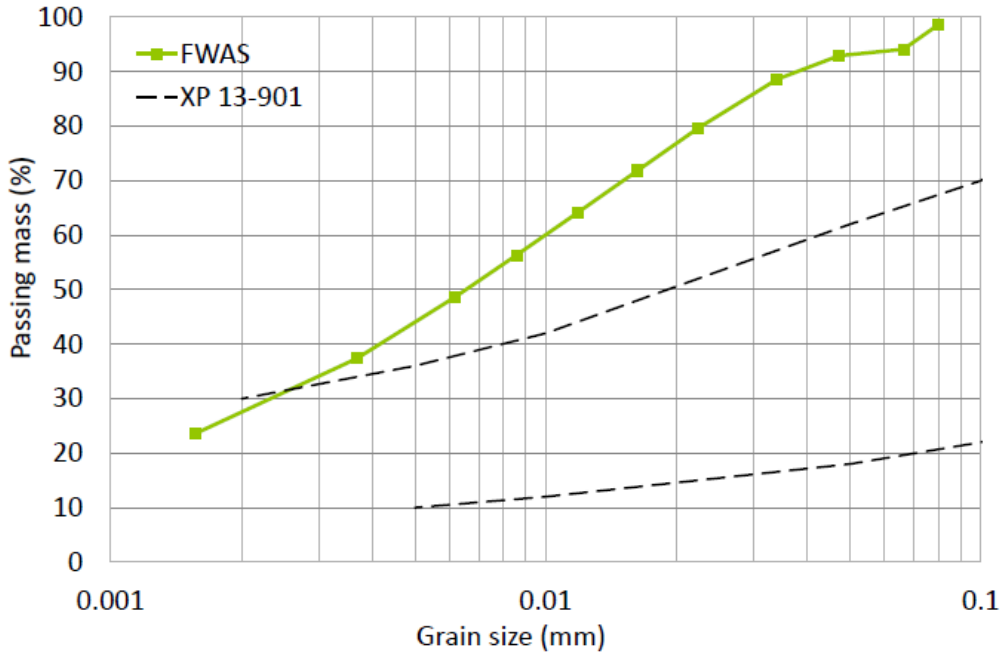


800
801

802 Figure 6. X-ray diffraction pattern of the earth.

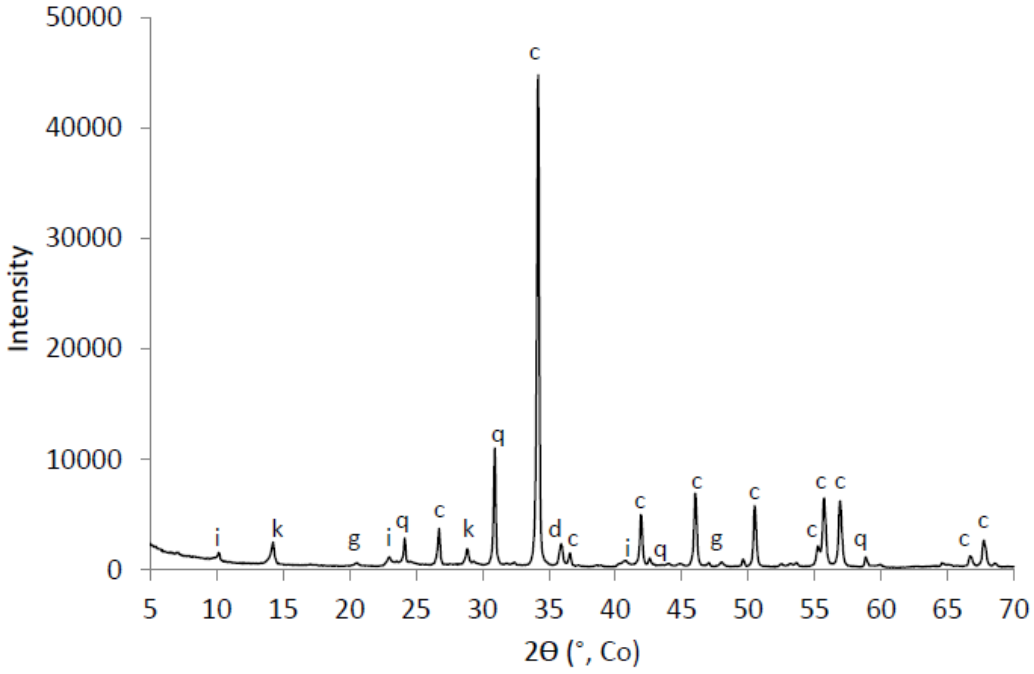


(c) calcite, (d) dolomite, (g) goethite, (i) illite, (k) kaolinite, (q) quartz

803
804

805 Figure 7. TG and DTG (Derivative Thermo-Gravimetric) curves of the earth

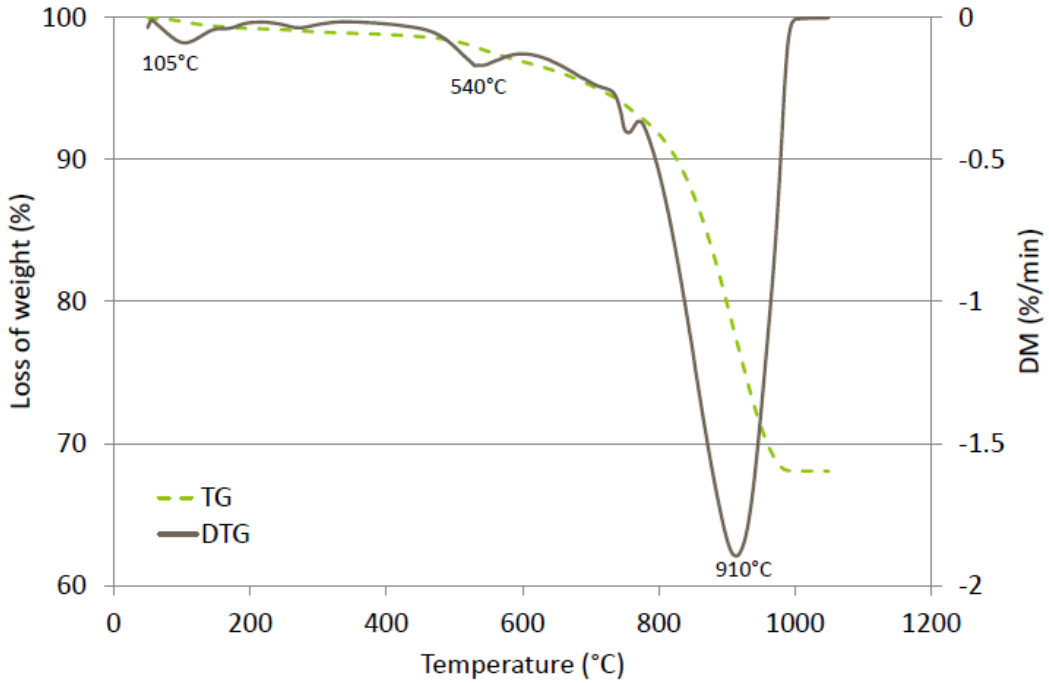


806
807

Figure 8. Bulk density as a function of the plant aggregate content

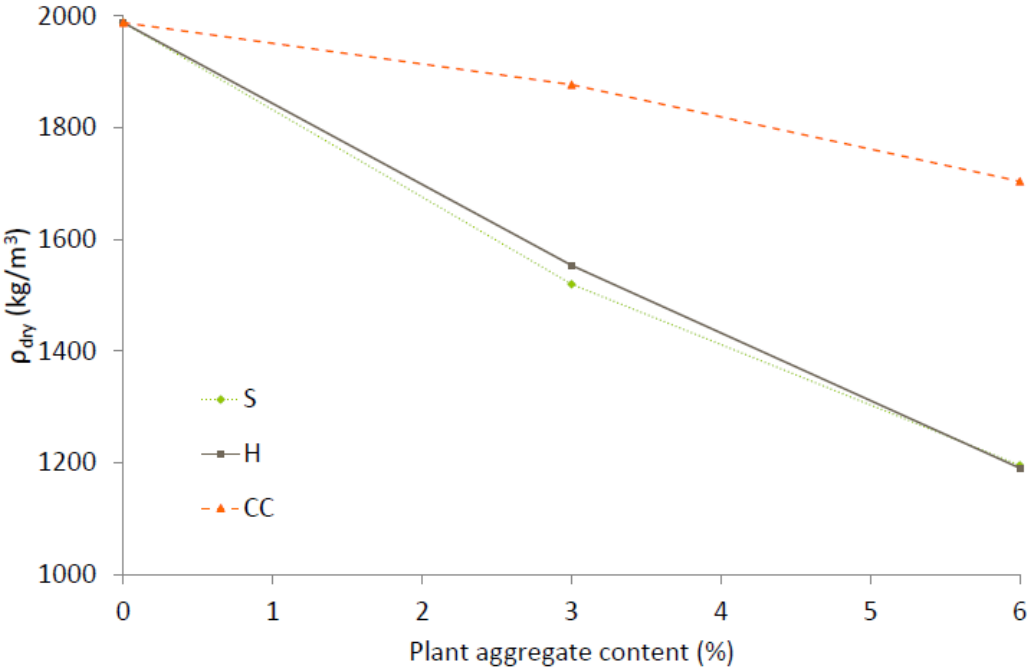

811 Figure 9. Compressive strength of the mixtures according to the testing protocol

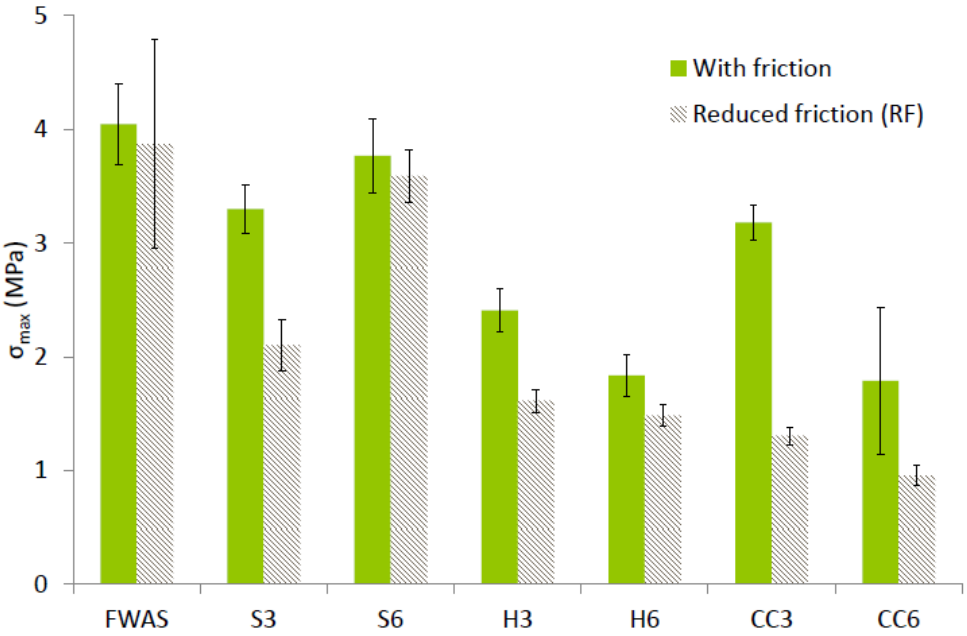


812
813

814 Figure 10. Results for compressive strength test with friction

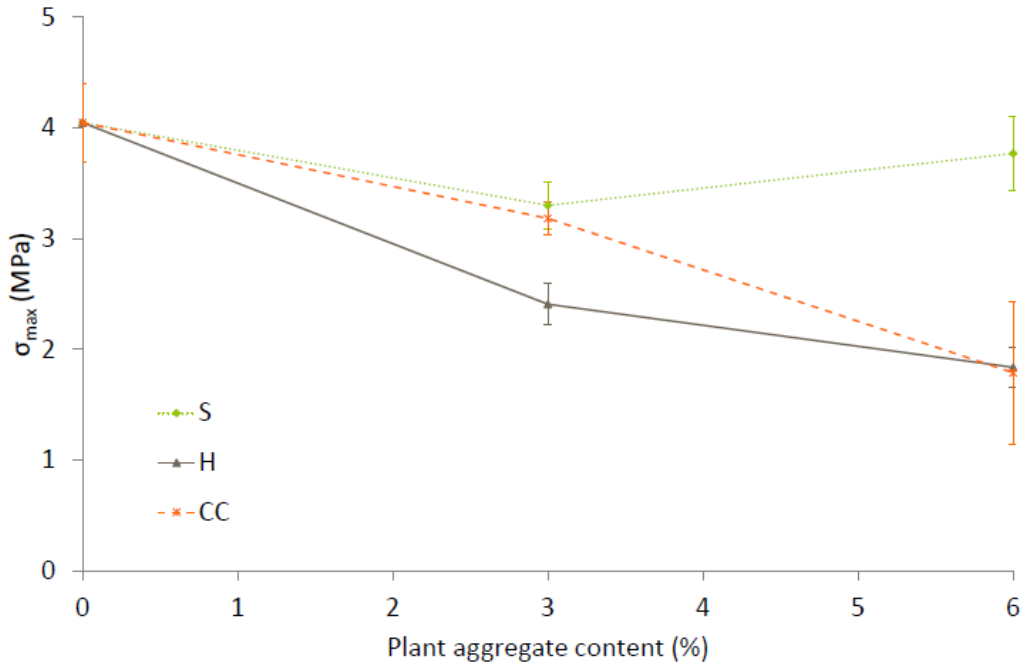


815
816

817 Figure 11. Strain-stress diagram for all the specimens

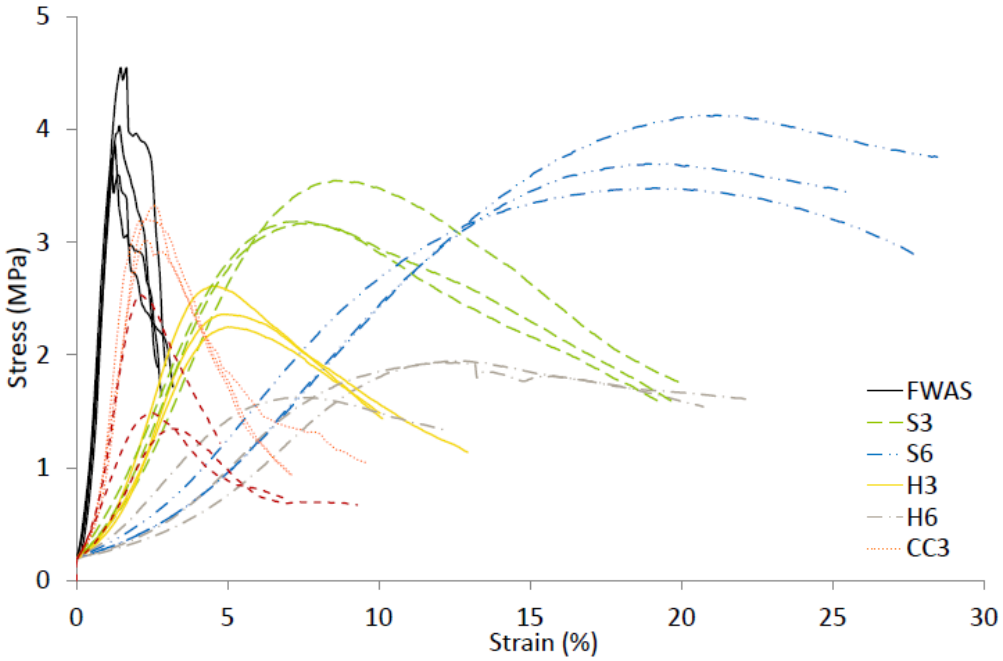


818
819

820 Figure 12. Maximum compressive strength ($\sigma_c$) and compressive strength at
821 1.5% strain ($\sigma_{c,1.5}$%)

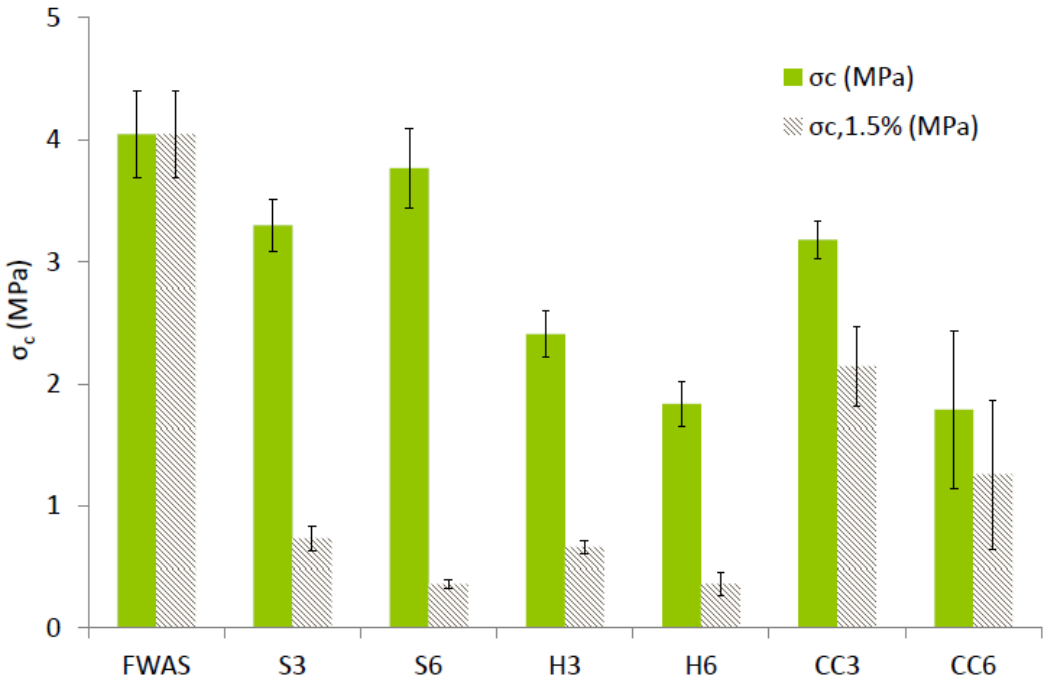


822
823

824 Figure 13. Young's moduli of the materials for both protocols

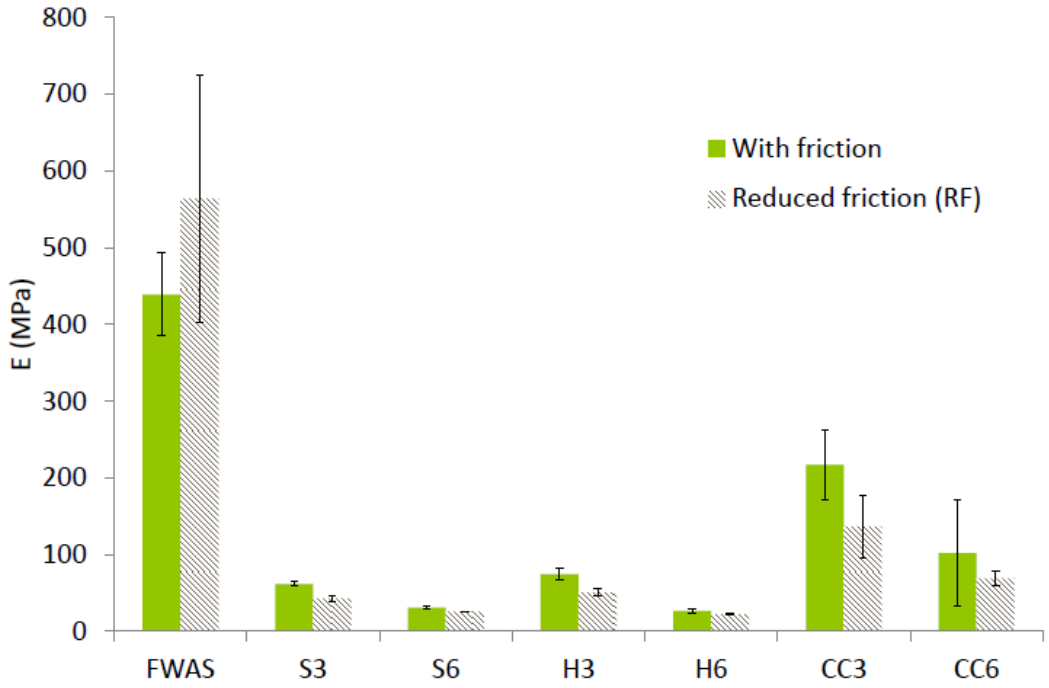


825
826

827 Figure 14. Young's modulus from compressive test as a function of the plant
828 aggregate content

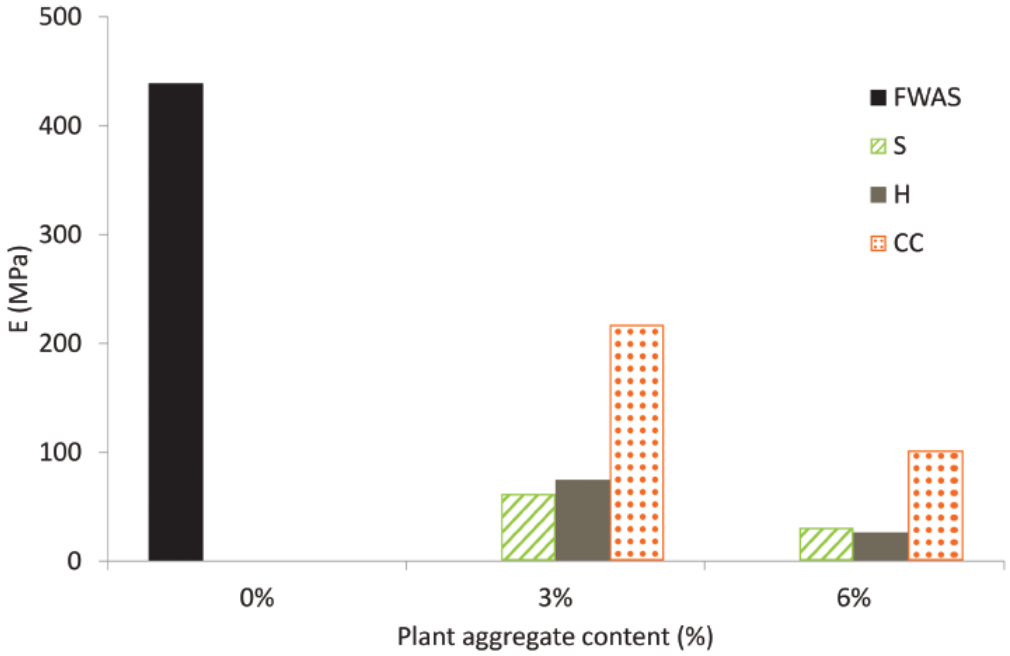


829
830

831 Figure 15. Young's modulus as a function of the density

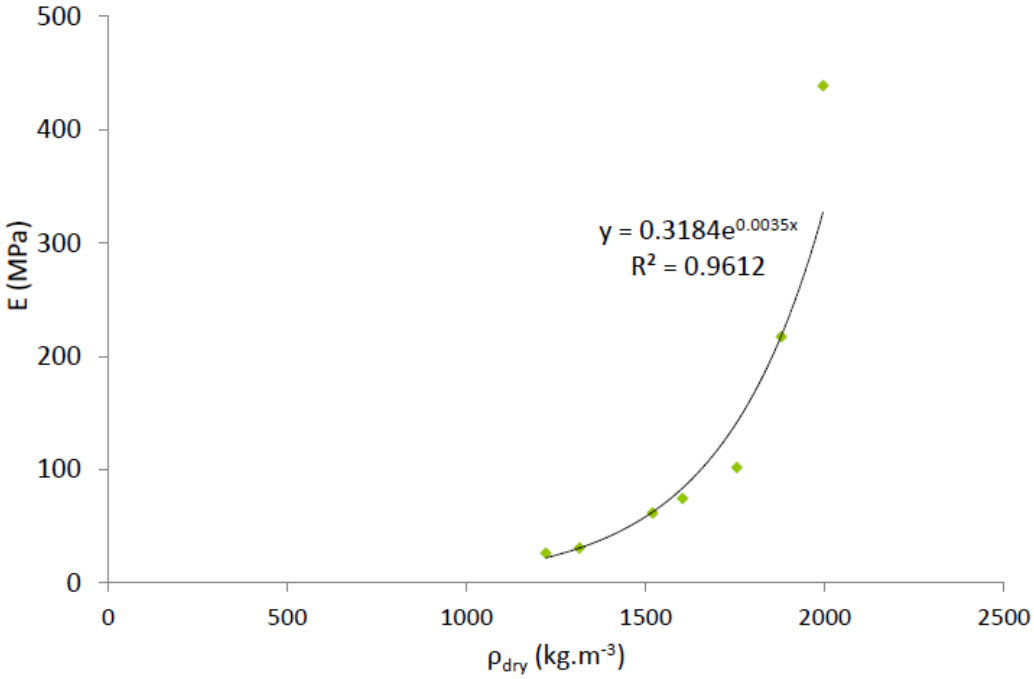


832
833

Figure 16. Influence of the plant aggregate on flexural behavior: (a) Flexural load-carrying capacity, (b) Peak strain ($\varepsilon_f$), (c) Average fracture energy ($G_f$) and (d) Young's modulus

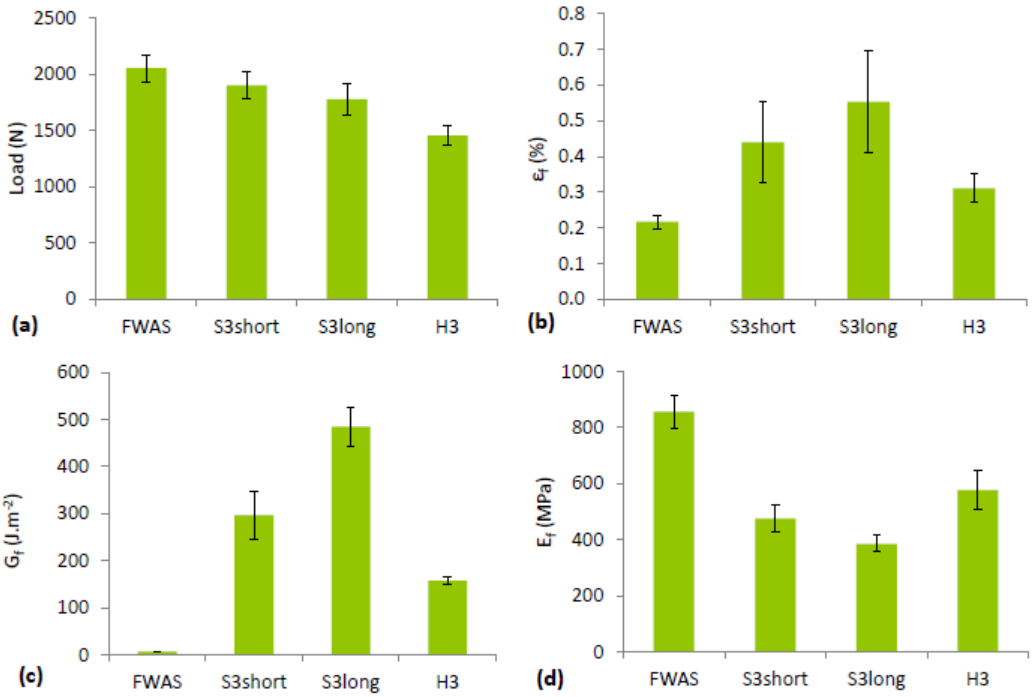

839 Figure 17. Typical load-deflection curves

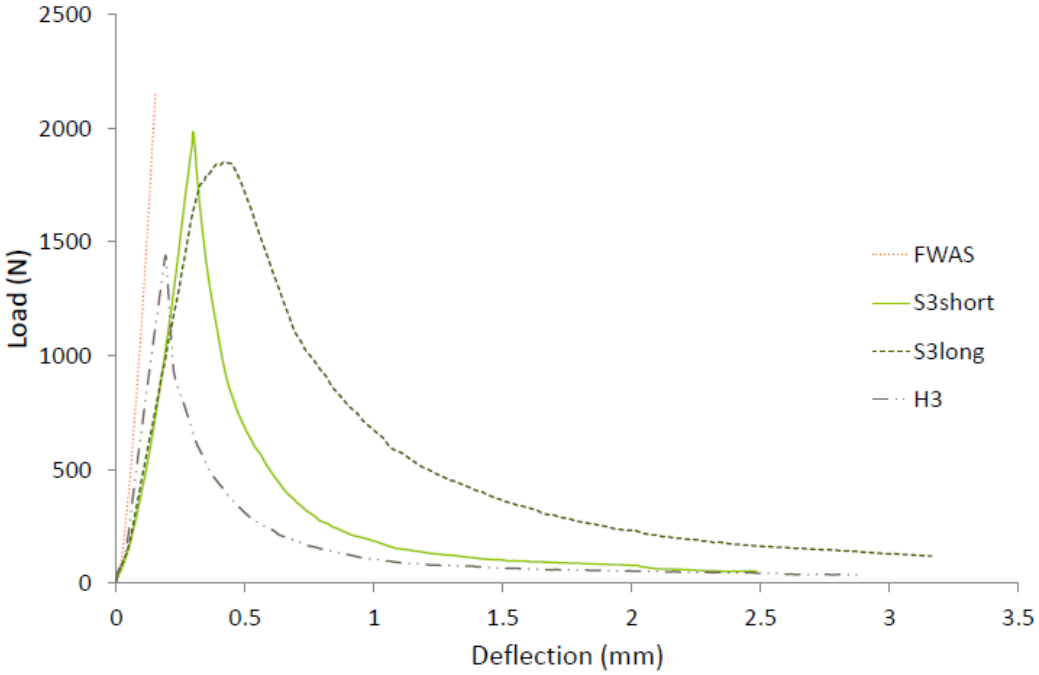


840
841

842 Figure 18. Influence of the surfactants on flexural behavior: (a) Flexural load-
843 carrying capacity, (b) Peak strain (εf), (c) Average fracture energy (Gf) and (d)
844 Young's modulus

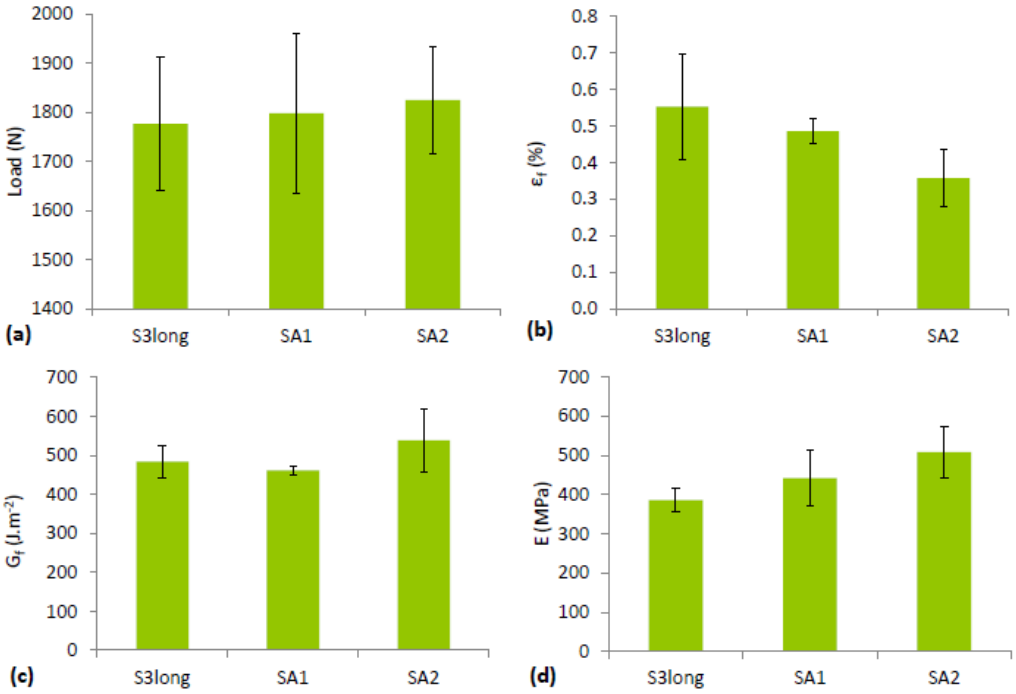


845